Branching Ratios of Excited Sn I States Produced by Collisions of $He(2^3S)$ Atom with $SnCl_4$ and $Sn(CH_3)_4$

Ikuo Tokue, * Yuko Sakai, Masaaki Kobayashi, and Katsuyoshi Yamasaki

Department of Chemistry, Faculty of Science, Niigata University, Ikarashi, Niigata 950-21

(Received May 7, 1996)

Fluorescence in the 200—600 nm range from excited fragments produced by collision of $He(2^3S)$ with $SnCl_4$ and $Sn(CH_3)_4$ has been studied in the relative collision energy of 135—210 meV. Emission cross sections for Sn I atomic resonance lines from $SnCl_4$ slightly decrease with increasing collision energy. This originates from the fact that the effective potential between $He(2^3S)$ and $SnCl_4$ is slightly attractive. The branching ratio of Sn I states observed from $SnCl_4$ is consistent with a simple dissociation model assuming equipartition of the available energy. These results are compatible with the harpoon mechanism as an initial step for formation of Sn I from $SnCl_4$. On the other hand, the effective potential between $He(2^3S)$ and $Sn(CH_3)_4$ is found to be repulsive, and the branching ratio of Sn I is increased to much more than that estimated from the statistical model. Excited Sn I states seem to be produced directly from $Sn(CH_3)_4$ by an excitation transfer mechanism via superexcited states, which mainly decay by Penning ionization.

The $He(2^3S$: 19.82 eV) atom, which has a large excitation energy and a long radiative lifetime, can excite a target molecule (M) to superexcited states. These states can mainly decay to either several ion states by Penning ionization ($He^* + M \rightarrow He + M^{*+} + e^-$) or neutral excited fragments via such a process, $He^* + M \rightarrow He + A + B^*$.

In Penning ionization of He^* atoms at very low energies, the total and state-resolved ionization cross sections decrease as the collision energy increases until about 100 meV where they begin to rise.[1—4] As the collision energy increases, the cross section reaches a maximum around 10 eV. The first decrease originates in the attractive potential well, while the increase is due to the repulsive part of the interaction potential. For neutral fragmentation resulting from collision of He^* with target molecules, very little is known about the dependence of their cross sections on the collision energy. Nevertheless, the general features observed in the dependence of Penning ionization cross sections can be applied to the dependence of the cross section for neutral fragmentation.

Formation of excited fragments resulting from the collisions of He^* atoms with molecules containing a group IV B atom has been studied by optical spectroscopy at thermal energy. Concerning tin compounds, Tsuji et al.[5—7] studied emissions produced from SnH_4 and $SnCl_4$ in the helium afterglow from an interest in the spectroscopy of ionic species. In the $He(2^3S) + SnCl_4$ reaction,[5] the Sn I and Sn II lines, and the SnCl(A–X) and SnCl(B–X) bands were observed. Nevertheless, there has been only a little information about the dissociation mechanism of target molecules containing a group IV B atom, especially at higher collision energies. The interaction of a target molecule with $He(2^3S)$ and its decay process are more complicated than that with a photon or an electron. Therefore, the knowledge of the interaction potential of the target molecule with $He(2^3S)$ is required for quantitative understanding of the dissociation dynamics.

This paper reports state-resolved emission cross sections of Sn I resonance lines and branching ratios of Sn I states observed from $SnCl_4$ and $Sn(CH_3)_4$ by using a crossed-beam method, and discusses the effective potentials with $He(2^3S)$ and the reaction dynamics of producing excited Sn I.

Experimental

The apparatus and experimental details for the fluorescence measurement have been reported previously.[8] In brief, $He(2^3S, 2^1S)$ atoms are produced with a nozzle discharge source[4] and skimmed into a collision chamber; the singlet component of the total He^* flux was estimated to be about 10%. Target gases flowed out to the collision chamber forming the effusive molecular beam through a multicapillary array. The pressure of the target gas was measured at the upper stream of the multicapillary array with an MKS Baratron (Model 122A). Under typical stable operating conditions, the discharge current was 10—30 mA, the voltage was 400—750 V, and the pressure of residual gas at the collision chamber measured by an ionization vacuum gauge was 2.7 mPa. The samples of $SnCl_4$(stated purity of 97%) and $Sn(CH_3)_4$ (stated purity of 95%) commercially obtained were used after degassing.

The fluorescence resulting from the collision of $He(2^3S)$ with target molecules was observed in a direction perpendicular to both the molecular and He^* beams. The relative sensitivity of the total photon-detection system was calibrated with a deuterium lamp in the 200—310 nm region and with a halogen lamp in the 310—600 nm region. In this study, the emission cross section (σ_{em}) for the fluorescence produced by collisions of $He(2^3S)$ was evaluated by comparing its emission intensity with that of the following Penning ionization:

$$He(2^3S) + N_2 \rightarrow N_2^+(B^2\Sigma_u^+) + He + e^- . \quad (1)$$

The $N_2^+(B^2\Sigma_u^+)$ state only radiates to the $N_2^+(X^2\Sigma_g^+)$ state and the σ_{em} of the N_2^+(B–X) band produced by reaction 1 then becomes equal to the partial cross section for the formation of the N_2^+(B) state. We

have adopted the σ_{em} value of $(3.2\pm0.3)\times10^{-20}m^2$ for reference reaction 1 at a relative collision energy (E_R) of 140 meV; this value was estimated from Fig. 5 in Ref. 9. The total emission intensity of the N_2^+(B–X) system was derived from the observed intensities of the 0–0 and 1–0 bands by using the scaling factors calculated by Comes and Speier.[10] The experimental errors attached to σ_{em} values are estimated to be 5—10%.

Velocity distributions of the He* beam were observed with a separate apparatus with a similar He* beam source by using the time of flight (TOF) method. The apparatus consists of a He* beam source, a collimation chamber, and a metastable atom detection chamber. The beam of metastable atoms was pulsed by a mechanical chopper rotating at 100 Hz in a collimation chamber. The velocity distribution of He* beam was obtained by measuring the TOF from the chopper disk to a plate (stainless steel) placed 810 mm downstream in the metastable atom detection chamber; secondary electrons produced from the plate were detected by a channel electron multiplier (Murata, Model EME-1061B). The TOF spectrum was recorded by a digital oscilloscope with a channel width of 1 μs and accumulated with a personal computer. The zero time was established by measuring light from the discharge region. The velocity distribution observed under typical discharge conditions could be represented by a Maxwell–Boltzmann distribution. The average kinetic energy (E_M) of the He* beam was found to depend only on the discharge power at the beam source; the E_M is derived from the root-mean-square velocity (v_M) of the He* beam. The E_M value thus derived almost coincides with the most probable energy for each TOF spectrum. Figure 1 shows the dependence of E_M and the beam width (HWHM) on the discharge power; HWHM was estimated from the half width half maximum of the velocity distribution.

In the fluorescence measurement, we could not use the chopped He* beam because of weak fluorescence intensity. Thus, we have controlled the kinetic energy of the He* beam by varying the discharge power, since E_M increases with the discharge power as shown in Fig. 1. Therefore, it should be stressed that σ_{em} values were measured with a relatively broad collision energy distribution.

The relative velocity averaged over the velocities of He* atom and the target molecule is expressed as

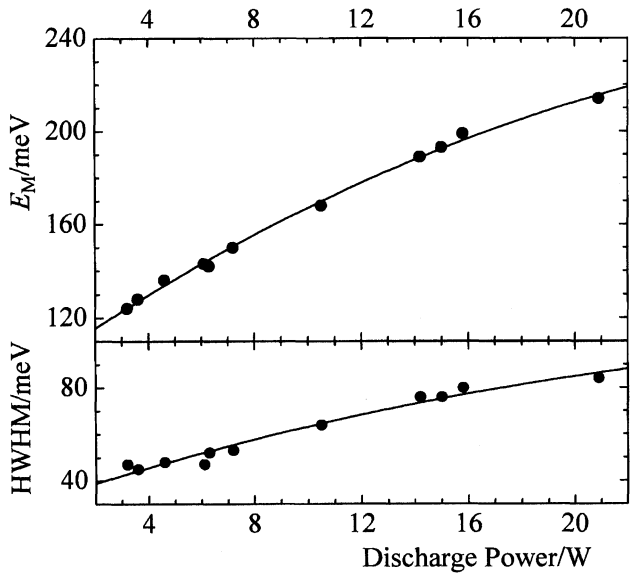

Fig. 1. Average kinetic energy (E_M) and half width half maximum(HWHM) of He* beam versus discharge power.

$$v_R = (v_M^2 + 3kT/m)^{1/2}, \quad (2)$$

where T and m are the temperature (300 K) and the mass of the target molecule, respectively. The collision energy dependence of σ_{em} was obtained by converting the function of E_M into that of E_R with the relation between E_R and the reduced mass (μ) of the He+target system;

$$E_R = \mu v_R^2/2. \quad (3)$$

Results

Branching Ratios of Excited Sn I States. Photoemissions in the 200—600 nm from excited fragments produced by collision of He(2^3S) with target molecules have been measured at the relative collision energy (E_R) of 135—210 meV. Figures 2 and 3 show fluorescence spectra in the 220—400 nm region produced from $SnCl_4$ and $Sn(CH_3)_4$, respectively, at E_R of 153 meV. Observed peaks from both molecules have been assigned as the Sn I resonance lines. No Sn II line was observed. In the assignment, we used transition frequencies and wavelengths for Sn I or Sn II resonance lines calculated from the electronic energies of corresponding Sn I or Sn II states.[11] From $SnCl_4$ a weak SnCl($A^2\Delta$–$X^2\Pi$) band was also observed, while no SnCl($B^2\Sigma^+$–$X^2\Pi$) band was detected.[5]

Table 1 lists relative intensities for the Sn I transitions observed from $SnCl_4$ and $Sn(CH_3)_4$. Other Sn I emissions that can affect the populations of the upper states for the observed 20 lines are very weak in the 200—600 nm range. Thus, we have concluded that cascading from higher states is negligible. When all emission lines from the upper state i of Sn I produced are measured, the relative population $N(i)$ for the i state can be evaluated by

$$N(i) \propto R(i) = \sum_j R_{ij}, \quad (4)$$

Table 1. Relative Intensities for Sn I Resonance Lines Produced from $SnCl_4$ and $Sn(CH_3)_4$

Transition	λ/nm	Relative intensity	
		$SnCl_4$	$Sn(CH_3)_4$
$5d\ ^3D_1 \rightarrow 5p^2\ ^3P_0$	224.63	No	0.668
$7s\ ^1P_1 \rightarrow 5p^2\ ^1D_2$	226.81	No	0.316
$5d\ ^3D_2 \rightarrow 5p^2\ ^3P_1$	235.49	0.139	1.592
$5d\ ^3D_3 \rightarrow 5p^2\ ^3P_2$	242.95	0.140	2.114
$5d\ ^3F_2 \rightarrow 5p^2\ ^3P_2$	248.34	0.049	0.697
$6s\ ^1P_1 \rightarrow 5p^2\ ^3P_0$	254.66	0.114	0.184
$6s\ ^1P_1 \rightarrow 5p^2\ ^3P_1$	266.13	0.046	0.080
$6s\ ^3P_2 \rightarrow 5p^2\ ^3P_1$	270.65	0.373	0.820
$5p^3\ ^5S_2 \rightarrow 5p^2\ ^3P_2$	276.18	0.624	0.608
$6s\ ^3P_2 \rightarrow 5p^2\ ^3P_2$	284.00	0.863	1.851
$5d\ ^3F_2 \rightarrow 5p^2\ ^1D_2$	285.06	0.079	0.878
$6s\ ^3P_1 \rightarrow 5p^2\ ^3P_0$	286.33	0.742	0.750
$6s\ ^3P_1 \rightarrow 5p^2\ ^3P_1$	300.92	0.462	0.443
$6s\ ^3P_0 \rightarrow 5p^2\ ^3P_1$	303.41	0.760	0.773
$6s\ ^3P_1 \rightarrow 5p^2\ ^3P_2$	317.50	1.000	1.000
$5p^3\ ^5S_2 \rightarrow 5p^2\ ^1D_2$	322.36	0.091	0.095
$6s\ ^1P_1 \rightarrow 5p^2\ ^1D_2$	326.23	0.464	0.945
$6s\ ^3P_2 \rightarrow 5p^2\ ^1D_2$	333.06	0.064	0.133
$6s\ ^3P_1 \rightarrow 5p^2\ ^1D_2$	380.10	0.169	0.157

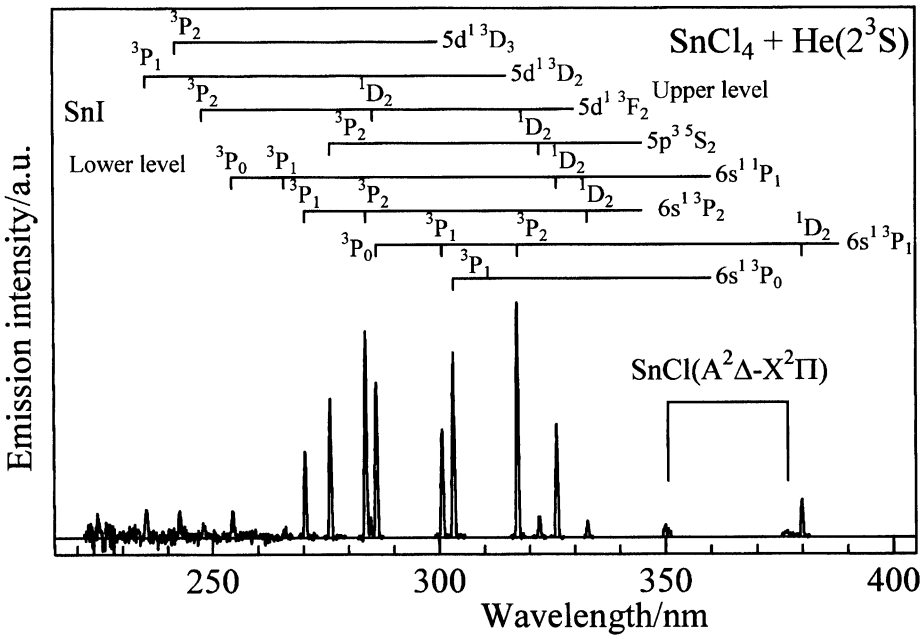

Fig. 2. Fluorescence spectrum resulting from collision of He(2^3S) with $SnCl_4$ at a relative collision energy of 153 meV with the optical resolution of 0.6 nm (fwhm); the optical sensitivity is calibrated.

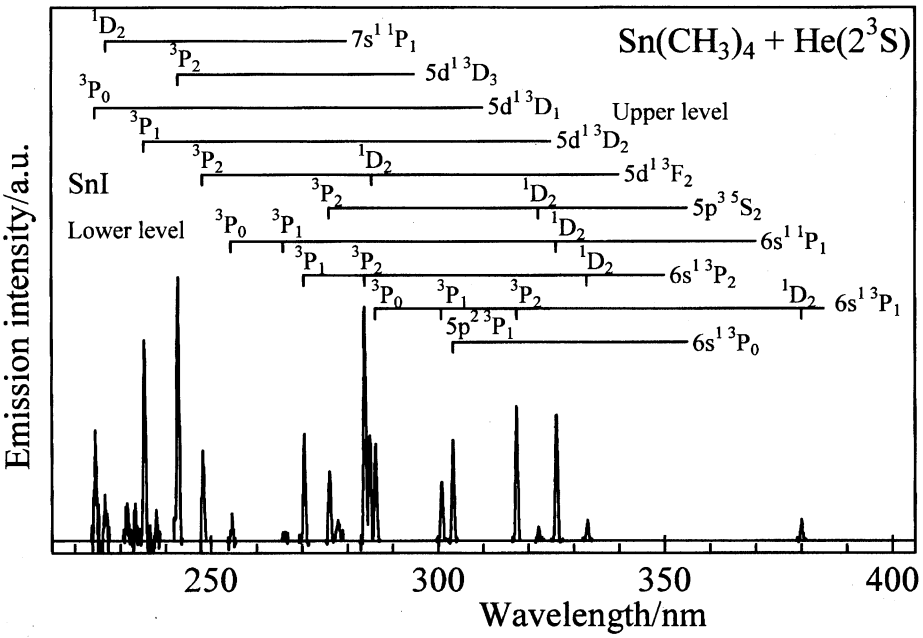

Fig. 3. Same as Fig. 2 but for $Sn(CH_3)_4$.

where R_{ij} is the emission intensity for the $i \rightarrow j$ transition and $R(i)$ represents the total emission intensity for the i state. The radiative lifetimes for the observed Sn I states are very short[12] so that the populations are not affected by the difference in the lifetime. Total emission intensity (R) of the Sn I states observed and their relative populations normalized by the degeneracy, $N/(2J+1)$, are listed in Table 2, and Fig. 4 shows the relative populations for the excited Sn I states against their electronic energies (E).

The populations of Sn I from $SnCl_4$ and $Sn(CH_3)_4$ were represented by Boltzmann temperatures (T_e) of 3950 ± 300 and 13300 ± 1200 K, respectively. On the assumption that these temperatures can be applied to the populations of all states of Sn I, the average electronic energy for Sn I (E_e) was evaluated by

$$E_e = \frac{\sum_i (2J_i+1)E(i)\exp[-E(i)/kT_e]}{\sum_i (2J_i+1)\exp[-E(i)/kT_e]}. \quad (5)$$

The E_e values thus obtained from $SnCl_4$ and $Sn(CH_3)_4$ are 0.28 ± 0.02 and 1.31 ± 0.12 eV, respectively.

Collision Energy Dependence of Emission Cross Sections. Total σ_{em}'s of Sn I lines in the 200—600 nm region produced by collision of He(2^3S) with $SnCl_4$ and $Sn(CH_3)_4$

Table 2. Total Emission Intensities (R) and Relative Populations (N) for the Excited Sn I States Produced from $SnCl_4$ and $Sn(CH_3)_4$

Upper state	E/eV[a]	τ/ns[b]	$SnCl_4$		$Sn(CH_3)_4$	
			R[c]	$N/(2J+1)$[d]	R[c]	$N/(2J+1)$[d]
$6s\ ^3P_0$	4.295	6.0	1.00	100	1.00	100
$6s\ ^3P_1$	4.329	4.8	3.10	103(12)	3.13	104(7)
$6s\ ^3P_2$	4.789	4.4	1.73	35(6)	3.66	73(2)
$6s\ ^1P_1$	4.867	4.5	0.82	27(4)	1.60	53(5)
$5d\ ^3D_2$	5.473	5.3	0.19	3.9(1.0)	1.93	38(6)
$5d\ ^3D_1$	5.518	4.1	—	—	0.90	30(3.5)
$5d\ ^3D_3$	5.527	5.8	0.18	2.6(0.6)	2.80	40(8)

a) The E is the electronic energy. b) The radiative lifetime; Ref. 12. c) Total emission intensity. d) The J is the total angular momentum and the numbers in parentheses mean the experimental errors.

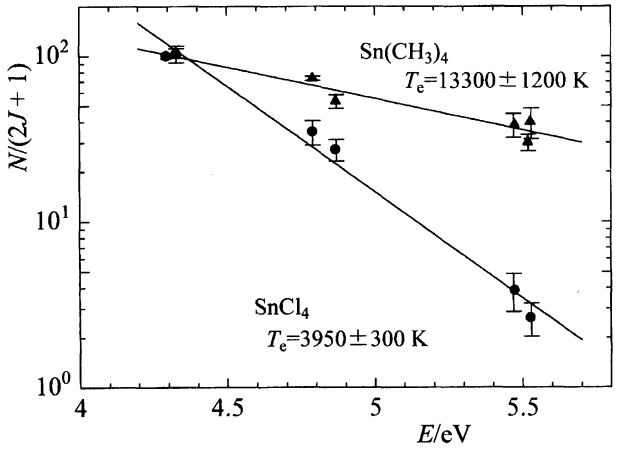

Fig. 4. Relative populations (N) for the excited Sn I states versus the electronic energy (E): the error bars represent twice the standard deviation.

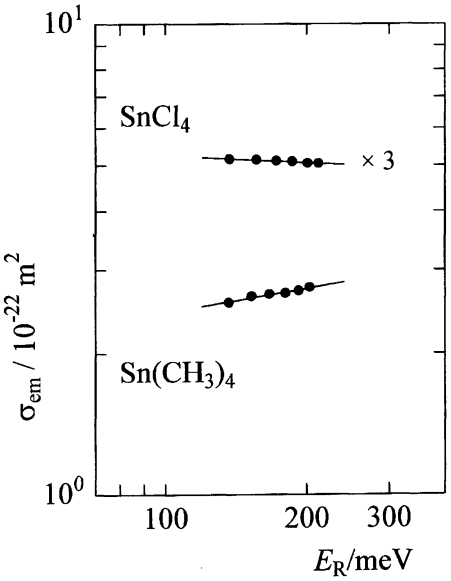

Fig. 5. Collision energy dependences of σ_{em} for the 317.5 nm line produced from collision of $He(2^3S)$ with $SnCl_4$ and $Sn(CH_3)_4$.

were evaluated to be 0.95 ± 0.11 and $(0.37\pm0.05)\times10^{-20}$ m^2, respectively. The σ_{em} for the SnCl(A–X) band was estimated to be smaller than 0.03×10^{-20} m^2. The relative populations of the excited Sn I states observed from both molecules, which are listed in Table 2, were nearly constant in the relative collision energy of 135—210 meV. Thus, the dependence of the total σ_{em} for Sn I lines on the collision energy (E_R) has been calculated by measuring the intensity of the strongest $6s\ ^3P_1 \rightarrow 5p^2\ ^3P_2$ line at 317.5 nm; other lines were too weak to measure the dependence. Figure 5 shows plots of $\log \sigma_{em}$–$\log E_R$ for collision energy dependences of σ_{em} for the 317.5 nm line produced from $SnCl_4$ and $Sn(CH_3)_4$. The observed data were fitted with the function of $\log \sigma_{em} = m \log E_R + C$,[4] and the slope m is evaluated to be -0.05 ± 0.03 for $SnCl_4$ and 0.17 ± 0.05 for $Sn(CH_3)_4$. The positive slope reflects the repulsive character of the effective potential between $He(2^3S)$ and the target molecule, while the negative slope originates in the attractive potential.

Discussion

By combining the thermochemical data[13] with the electronic energy of $He(2^3S)$, 19.82 eV, formation processes for the ground state of Sn I that are energetically possible from $SnCl_4$ and $Sn(CH_3)_4$ are as follows:

$$He(2^3S) + SnCl_4 \rightarrow Sn(5p^2\ ^3P_0) + 4Cl + He + 6.76\ eV, \quad (6)$$

$$He(2^3S) + SnCl_4 \rightarrow Sn + 2Cl + Cl_2 + He + 9.28\ eV, \quad (7)$$

$$He(2^3S) + Sn(CH_3)_4 \rightarrow Sn + 4CH_3 + He + 10.45\ eV, \quad (8)$$

$$He(2^3S) + Sn(CH_3)_4 \rightarrow Sn + 2CH_3 + C_2H_6 + He + 14.35\ eV, \quad (9)$$

where by-products are in the ground state.

The average electronic energies for Sn I (E_e) obtained from both molecules have been compared with the values estimated from equipartition of the available energy (E_{av}) among all degrees of freedom on the assumption that reactions 6—9 proceed via an intermediate complex between $He(2^3S)$ and the target molecule. For example, E_{av} of 6.76 eV for process 6 is distributed statistically among 19 degrees of freedom, neglecting the electronic energy of four Cl atoms; 18 degrees of freedom is for translational and one for the electronic energy of Sn I. Table 3 lists the estimated values for the average energy of Sn I (E_{av}/g) comparing with E_e. The E_e obtained from $SnCl_4$ is 80% of the E_{av}/g value for process 6, while E_e from $Sn(CH_3)_4$ is an order of

Table 3. Dissociation Processes of $SnCl_4$ and $Sn(CH_3)_4$ and Comparison of E_e with the Estimated (E_{av}/g) by a Statistical Model

Target	E_e/eV	Process[a)]	E_{av}/eV	g[b)]	(E_{av}/g)/eV
$SnCl_4$	0.28	6	6.76	19	0.356
		7	9.28	20	0.464
$Sn(CH_3)_4$	1.31	8	10.45	79	0.132
		9	14.35	85	0.169

a) Process is described in the text. b) The g value means total degrees of freedom; as for process 8, $g=3\times6$(translational) $+3\times4$(rotational)$+2\times6\times4$(vibrational)$+1$(electronic).

magnitude larger than the E_{av}/g values for processes 8 and 9. The result for $SnCl_4$ indicates that process 6 proceeds via a reaction intermediate and that the available energy is distributed approximately among all degrees of freedom. Although we cannot exclude process 7 thermochemically, the broad $Cl_2(D'-A')$ band, which was observed from the collisions of $He(2^3S)$ with CCl_4 and $GeCl_4$,[14—16] may appear near 258 nm in the case of process 7. The absence of the $Cl_2(D'-A')$ emission is probably caused by the fact that the Cl···Cl distance of $SnCl_4$, 0.372 nm,[17] is far longer than the equilibrium bond length for $Cl_2(D')$ 0.287 nm.[18] It can be concluded that process 7 is unimportant. On the other hand, dissociation of $Sn(CH_3)_4$ turns out to be direct and the internal degrees of freedom for CH_3 by-products should be frozen.

From the thermochemical viewpoint, excited Sn II states which fluoresce in the 200—600 nm cannot be produced from $SnCl_4$, while their formation is possible for $Sn(CH_3)_4$. Nevertheless, no Sn II emission was observed from both molecules.

The σ_{em} of the Sn I line from $Sn(CH_3)_4$ slightly increases with the collision energy. This is ascribed to the fact that the effective potential of $He(2^3S)$ with $Sn(CH_3)_4$ is slightly repulsive. In $He(2^3S)$ Penning ionization of $C(CH_3)_4$, Takami et al.[19] have reported that all partial Penning ionization cross sections increase with the collision energy; among the curves with positive slopes in the $\log\sigma$–$\log E$ plots, the slope for the C 2s ($4a_1$) band was found to be smaller than the others. The electron exchange model was succeeded in explanation of the probability for partial Penning ionization observed by Penning ionization electron spectroscopy (PIES)[20] and its collision energy dependence;[19] the positive slope for the partial Penning ionization cross sections of $C(CH_3)_4$ is briefly ascribed to the repulsive character between $He(2^3S)$ and CH_3 chromophore. Although very little is known about PIES of $Sn(CH_3)_4$, the interaction between $He(2^3S)$ and CH_3 chromophore seems to be similar to that for $C(CH_3)_4$. Nevertheless, the simple electron exchange model for Penning ionization cannot describe neutral fragmentation of $Sn(CH_3)_4$ induced by collision with $He(2^3S)$.

The excitation transfer is concluded to be involved in the C 2s band of $C(CH_3)_4$ from the estimation that the orbital energy of the $3a_1$(C 2s) orbital for $C(CH_3)_4$ is nearly equal to that of He 1s orbital.[19] The transition probability for this type of autoionization does not crucially depend on the distance between $He(2^3S)$ and target molecule. Thus, this mechanism explains the flattened collision energy dependence of the ionization cross section for the C 2s band.[19] The slope for the Sn I line observed from $Sn(CH_3)_4$, 0.17, is similar to that for the C 2s band and is smaller than the slopes for other bands in Penning ionization of $C(CH_3)_4$; the latter slopes can be estimated from Fig. 7 in Ref. 19. Although there is very little experimental and theoretical data on the orbital energies for $Sn(CH_3)_4$, the excitation transfer mechanism can explain the neutral fragmentation of $Sn(CH_3)_4$; by analogy with $C(CH_3)_4$, the Sn 5s orbital is probably a candidate for the orbital that strongly interacts with He 1s orbital. Some superexcited state of $Sn(CH_3)_4$ produced by electron transfer with $He(2^3S)$ can be followed by predissociation correlating with formation of Sn I on competing with autoionization, which is the main decay channel.

For the $He(2^3S)$ and $Sn(CH_3)_4$ system, even if products are branched into ionic states for Penning ionization and neutral fragments for dissociation in exit channels, the entrance potential surface is considered to be the same. This does not necessarily mean that the effective slope obtained for the Sn I line becomes the same as for final ionic states, which may be observed by PIES. The slope obtained for the Sn I line should be considered as a parameter reflecting effective distance where electronic transitions correlating with formation of Sn I occur. Although this distance between $He(2^3S)$ and $Sn(CH_3)_4$ is longer than the classical turning point, the effective potential is likely to become rather repulsive.

The σ_{em} of the Sn I line produced from $SnCl_4$ decreases slightly with increasing the collision energy. It becomes evident that the effective potential of $He(2^3S)$ with $SnCl_4$ is slightly attractive. The effective potential originates mainly in the long-range dispersion force. This trend with consideration on the average electronic energy of Sn I is compatible with the reaction scheme that formation of Sn I from $SnCl_4$ is initiated via a harpoon mechanism.[21] On the other hand, in a PIES study of $He(2^3S)$ with $C(CH_3)_3Cl$,[19] the $7e(n_{Cl})$ bands shows negative collision energy dependence, which can be related to the attractive nature of the interaction potential surface peculiar to the geometrical situations where the $He(2^3S)$ atom approaches the Cl atom of the target molecule. Therefore, the negative collision energy dependence of σ_{em} for the Sn I line from $SnCl_4$ can be attributed to the attractive nature between $He(2^3S)$ and Cl chromophore. Thus, two possible mechanisms (harpoon mechanism or excitation transfer mechanism) are compatible with the initial step for formation of Sn I from $SnCl_4$. Although it is not clear which mechanism is suitable as the initial step, we have estimated the total quenching cross section of $He(2^3S)$ with $SnCl_4$ on the assumption that the former is the dissociation model.

The first stage of the harpoon mechanism is described as the transfer of a 2s electron of $He(2^3S)$ to a vacant outer orbital of $SnCl_4$. The resulting attractive Coulomb force brings a produced ion pair together. The potential surface of the ion pair will be crossed over with several surfaces correlating to formation of excited Sn I at finite separation.

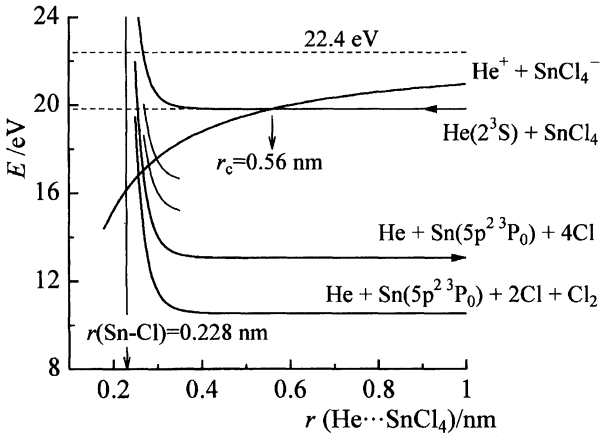

Fig. 6. Schematic diagram of interaction potentials between He and $SnCl_4$ and a dissociation scheme by the harpoon mechanism.

In this case, the cross section of quenching processes can become large and independent of the collision energy since the reaction has no threshold energy. Figure 6 shows schematically formation of Sn I resulting from collision of $SnCl_4$ with $He(2^3S)$ via the harpoon mechanism. The intermolecular distance between $SnCl_4$ and $He(2^3S)$, where the potential surface of $He(2^3S)+SnCl_4$ crosses with that of $He^+ + SnCl_4^-$ is estimated from the following assumptions:

(i) the attractive potential between the ion pair is approximated by a Coulomb force,

(ii) the repulsive and long-range attractive potentials between $He(2^3S)$ and $SnCl_4$ are neglected.

Taking into account of the ionization potential of $He(2^3S)$ 4.77 eV and the adiabatic electron affinity of $SnCl_4$, 2.2 eV,[22] the crossing point (r_c) is estimated to be 0.56 nm. The repulsive part of the potentials can be neglected at such a long distance since the Sn–Cl bond length is 0.228 nm.[17] The quenching cross section estimated from the relation, $\pi r_c^2/2$, is 49×10^{-20} m^2. On comparing with the total σ_{em} observed in the 200—600 nm region, the branching ratio for emission is estimated to be 1/50. Thus, decay channels for formation of excited fragments turn out to be very minor among the quenching processes of $He(2^3S)$ with $SnCl_4$. The ratio of transfer from the potential surface of the ion pair to decay channels is probably small. This small ratio for the dissociation process may be concluded also from the excitation transfer mechanism; excitation transfer processes followed mainly by autoionization, and predissociation should be minor.

We have concluded that the measurement of collision energy dependence of emission cross sections for excited fragments is successful for studying the interaction potential correlating with neutral dissociation. The knowledge concerning interactions of a 2*s* electron of He with vacant orbitals of a tin atom, especially 5*d* orbitals, seems to be important for further discussion on dissociation dynamics of $SnCl_4$ and $Sn(CH_3)_4$.

We are grateful to Dr. H. Yamakado of Tohoku University for helpful suggestions on the TOF measurement. This work has been partly supported by a Grand-in-Aid for Scientific Research from the Ministry of Education, Science and Culture.

References

1) J. T. Moseley, J. R. Peterson, D. C. Lorents, and M. Hollstein, *Phys. Rev. A*, **6**, 1025 (1972).
2) R. E. Olson, *Phys. Rev. A*, **6**, 1031 (1972).
3) A. Niehaus, *Ber. Bunsenges. Phys. Chem.*, **77**, 632 (1973).
4) K. Ohno, T. Takami, K. Mituke, and T. Ishida, *J. Chem. Phys.*, **94**, 2675 (1991).
5) M. Tsuji and Y. Nishimura, *Chem. Phys. Lett.*, **83**, 483 (1981).
6) S. Yamaguchi, H. Obase, M. Tsuji, and Y. Nishimura, *Chem. Phys. Lett.*, **119**, 477 (1985).
7) S. Yamaguchi, H. Obase, M. Tsuji, and Y. Nishimura, *Can. J. Phys.*, **64**, 700 (1986).
8) I. Tokue, T. Kudo, and Y. Ito, *Chem. Phys. Lett.*, **199**, 435 (1992).
9) R. A. Sanders, A. N. Schweid, M. Weiss, and E. E. Muschlitz, Jr., *J. Chem. Phys.*, **65**, 2700 (1976).
10) F. J. Comes and F. Speier, *Chem. Phys. Lett.*, **4**, 13 (1969).
11) C. E. Moore, "Atomic Energy Levels III," Nat. Stand. Ref. Data Ser., U. S. Government Printing Office, Washington (1971), p. 74.
12) A. A. Radzig and B. M. Smirnov, "Reference Data on Atoms, Molecules, and Ions," Springer-Verlag, Berlin (1985), p. 242.
13) D. D. Wagman, W. H. Evans, V. B. Parker, R. H. Schumm, I. Halow, S. M. Bailey, K. L Churney, and R. L. Nuttall, *J. Phys. Chem. Ref. Data*, **11**, No. 2 (1982).
14) M. Tsuji, T. Mizuguchi, and Y. Nishimura, *Chem. Phys. Lett.*, **84**, 321 (1981).
15) M. Tsuji, T. Mizuguchi, K. Shinohara, and Y. Nishimura, *Can. J. Phys.*, **61**, 838 (1983).
16) I. Tokue, H. Tanaka, and K. Yamasaki, (to be published).
17) H. Fujii and M. Kimura, *Bull. Chem. Soc. Jpn.*, **43**, 1933 (1970).
18) P. C. Tellinghuisen, B. Guo, D. K. Chakraborty, and J. Tellinghuisen, *J. Mol. Spectrosc.*, **128**, 268 (1988).
19) T. Takami, K. Mitsuke, and K. Ohno, *J. Chem. Phys.*, **95**, 918 (1991).
20) K. Ohno, H. Mutoh, and Y. Harada, *J. Am. Chem. Soc.*, **105**, 4555 (1983).
21) R. D. Levine and R. B. Bernstein, "Molecular Reaction Dynamics and Chemical Reactivity," Oxford Univ. Press, Oxford (1987).
22) K. Lacman, M. J. P. Maneira, A. M. C. Moutinho, and U. Weigmann, *J. Chem. Phys.*, **78**, 1767 (1983).